



Fermi National Accelerator Laboratory

TM-1572

**Main Ring Bunch Spreaders:
Past, 1987/1988 Fixed Target Run,
and Proposed Future***

Gerald P. Jackson
Fermi National Accelerator Laboratory
P.O. Box 500, Batavia, Illinois

February 26, 1989



Operated by Universities Research Association, Inc., under contract with the United States Department of Energy

MAIN RING BUNCH SPREADERS:
PAST, 1987/1988 FIXED TARGET RUN, AND PROPOSED FUTURE

Gerald P. Jackson

February 26, 1989

Abstract

During the last 1987/1988 fixed target running period beam intensity was limited many times by coherent instabilities in both the Main Ring and in the Tevatron. The intensity thresholds for instabilities are generally inversely proportional to the proton bunch length. Since fixed target operations are insensitive to the longitudinal phase space emittance of the beam, bunch spreaders are employed to increase this emittance, and hence the bunch length. As a result, more beam intensity can be delivered to the fixed target experiments.

This paper starts with a short history behind the old Main Ring bunch spreader. After discussing the physics of stimulated emittance growth, the design and performance of the 1987/1988 fixed target run Main Ring bunch spreader is discussed. Finally, designs of improved Main Ring and Tevatron bunch spreaders for the next fixed target run are proposed.

Old Bunch Spreader

Design

Besides some private notes kept by H. Miller, the only documentation on the design of the old Main Ring bunch spreader is in the form of an appendix in an internal Fermilab accelerator experiment report.¹ Figure 1 is a reproduction of the circuit block diagram from that report.

After the beam accelerates beyond the transition energy of the Main Ring it is generally undergoing both dipole and quadrupole synchrotron oscillations. The dipole (center of mass) oscillations are damped by the radial position feedback loops in the RF system. Quadrupole (or bunch length) oscillations are damped due to the dependence of synchrotron tune on synchrotron oscillation amplitude. Within a couple of these damping times, at approximately 400 ms after transition, the bunch spreader is engaged for 400 ms.

Assume that the longitudinal distribution of the beam is Gaussian (this simplifies the arguments but does not change the basic idea). The voltage waveform induced in the E-49 coaxial direction coupler has a positive going component which is also Gaussian. Therefore, the diode peak detector stores the peak voltage, which is inversely proportional to the bunch length and proportional to the beam intensity. The small amplitude synchrotron frequency at this time was roughly 200 Hz. Therefore, the diode peak detector saw a dominant frequency at 400 Hz. By filtering away extraneous signals (such a residual dipole and sextupole frequencies), a clean 400 Hz wave in phase with the beam quadrupole oscillation should appear at the input to the gain control.

The bandwidth of this 400 Hz wave is determined by the decoherence time of the quadrupole oscillation. Figure 2 is also reproduced from the above report, and shows various signal waveforms throughout the bunch spreader circuit when the intensity is 1.6×10^{13} protons. Of present

1. S. Ohnuma, F. Turkot, S. Pruss, H. Miller, and R. Gerig, "Longitudinal Phase Space Area of the Beam and the Bunch Spreader in the Main Ring", EXP-86 (September 28, 1977).

concern is the top photograph. which shows the quadrupole oscillation diminishing to $1/e$ of its transition induced amplitude in about 200-400 ms. This means that the bandwidth of the quadrupole oscillation frequency is roughly 1 Hz.

After the gain and phase controls, the 400 Hz wave is gated and limited. The limiter is necessary since this signal is going to be used to excite an even larger quadrupole oscillation. Due to the positive feedback nature of this signal, a limiter prevents an uncontrolled, exponential growth in the bunch quadrupole oscillation. Finally, the limited signal is fed into the RF phase shifter control input, shaking the beam phase at twice the synchrotron frequency (400 Hz). In an accelerating RF wave, the longitudinal restoring force is a function of the longitudinal position of the bunch with respect to the RF waveform. Therefore, varying the RF phase at twice the synchrotron frequency induces longitudinal phase space mismatches at twice the synchrotron frequency, causing quadrupole oscillations. The rest of the photographs in figure 2 show the voltage waveforms throughout the circuit path.

Past Performance

The emittance growth performance of the old Main Ring bunch spreader was documented for small initial longitudinal emittances (0.045 eV-sec) in the above report, and also for larger initial emittances (0.37 eV-sec).² The bunch 90% emittance was measured by decreasing the RF voltage to various levels, recording the charge transmission, and extrapolating to the bucket area in which 90% of the beam survived. At an intensity of 3×10^{12} protons the longitudinal emittance was increased from 0.045 to 0.25 eV-sec. At an intensity of 2×10^{13} protons the emittance increased from 0.37 to 0.51 eV-sec.

Clearly the spreader did increase the beam emittance. But a side effect of the bunch spreader was beam intensity loss. The understanding

2. S. Ohnuma, H. Miller, J. Liebau, S. Pruss, and F. Turkot, "Longitudinal Phase Space Area of the Beam in the Main Ring", EXP-87 (March 22, 1978).

of the relationship between spreading efficiency and beam loss was referred to as:³

" A complicated interaction exists between the various bunch spreader adjustments, main-ring intensity, and available rf accelerating voltage. Up to now, a mystical approach has been used to set bunch spreader gain which has always been a compromise between adequate bunch spreading for extraction and beam loss due to an apparent lack of rf voltage."

In addition, a close examination of the top photograph in figure 2 yields a large amount of information not discussed in the reference. First, between transition and the start of bunch spreading the average bunch length is clearly increasing. This is due to the decoherence of the coherent quadrupole oscillation into increased longitudinal emittance, and hence increased average bunch length.

Second, 110 ms after the bunch spreader start gate, there was a discontinuous drop both in the average diode detector output voltage and the rms variation in that signal. Either a large percentage of the coherent bunch length oscillation was instantaneously converted into emittance, or there was a fast beam intensity loss mechanism which scraped away that percentage of the beam undergoing the dominant portion of the quadrupole oscillation. Either way, it is clear that such sudden changes are not consistent with the theory behind the bunch spreader design.

Finally, after this sudden event, notice that although a sizeable bunch length oscillation (comparable to the oscillation after transition) is taking place, there is no apparent emittance growth.

1987/1988 Fixed Target Run Performance

During the 1987/1988 fixed target run an intensity limit presumably due to a coherent instability became evident in the Tevatron. While trying to diagnose the problem in the Tevatron, the pulse to pulse

3. H. Miller, EXP-86 (Appendix).

variation in longitudinal emittance coming out of the Main Ring made quantitative studies impossible. In the process of investigating the source of this variation, it was noted that the Main Ring bunch spreader was causing coherent bunch length oscillations, but not consistent longitudinal emittance growth. Figure 3 contains a photograph of a signal similar to that generated by the diode peak detector while the bunch spreader was active. Note that the average voltage (and hence longitudinal emittance) does not change.

Finally, an inconvenient compromise was required between spreading efficiency and radial offset (beam momentum) feedback gain. By lowering the radial gain, the bunch spreader was significantly more effective at bunch lengthening. Unfortunately, since the radial offset feedback was basically disabled, the radial offset of the bunch varied, with resultant betatron tune, chromaticity, and coupling variations.

On the basis of these observations, the study of bunch spreaders in the Main Ring recommenced. The first steps of this study were the investigation of bunch spreader physics and the construction of a new spreader circuit.

Bunch Spreader Physics

Bunch Length Measurements

Much of the discussion in this document relies on measurements of bunch length. Therefore, it is important to discuss the types of bunch length detectors used in the past and at present.

In the old bunch spreader the bunch length (and the phase of the quadrupole oscillation) was measured using a diode peak detector connected to a beam detector. Figure 4 shows a mountain range example of a typical bunch profile. Note that even though the low frequency shape of the bunch appears Gaussian, there is enough noise to make any peak detector bunch length measurement unreliable.

But what aspect of the longitudinal bunch profile are we really interested in monitoring? As stated before, the purpose of the bunch

spreader is to diminish the severity of coherent instabilities. If the instability is due to a broad band resonator, then its growth rate would decrease as the bunch length is increased. If the instability is due to a single, narrow band resonator, then the frequency component of the bunch profile at that frequency is the important quantity, independent of the bunch length directly.

In the latter case, unless one knows the particular frequencies of interest, not much can be done in the way of meaningful measurements. On the other hand, it is possible to make a comparative estimate of the growth rate of such an instability by monitoring the bunch length. Assume that the bunch profile starts out as a smooth Gaussian, with σ the temporal bunch length. The Fourier transform of such a density distribution, in the range of bunch lengths of interest for the Main Ring, yields the frequency spectrum

$$I(\omega) = I_0 e^{-\omega^2 \sigma^2 / 2} \quad (1)$$

Clearly, the longer the bunch the less spectral power at any given frequency. Since the growth rate of a particular frequency in the bunch profile generally scales with the original spectral power at that frequency, it is possible to reduce the severity of, or even eliminate, the eruption of a coherent instability later in the beam acceleration cycle.

Therefore, a low noise signal is required which gives bunch length information. During fixed target operations the dominant frequency component of the bunch profile is at the RF frequency of 53 MHz. Passing a beam detector output signal through a narrow RF frequency bandpass filter generates a signal proportional to $I(\omega)$ which is devoid of the high frequency noise which plagued the old bunch spreader. This signal, called M:BPD in the Fermilab control system, is presently in use as a beam diagnostic.

Physics of Emittance Growth

For bunches whose length is much less than the RF period, the 90% invariant longitudinal phase space emittance (ϵ) is approximately

$$\epsilon = \frac{6 \pi \Omega E}{\eta} \sigma^2, \quad (2)$$

where Ω is the small amplitude angular synchrotron frequency, E is the beam energy, and η is the momentum compaction. The momentum compaction is a function of energy, and the synchrotron frequency is a function of both energy and RF voltage. Therefore, bunch lengthening at a given energy and RF voltage is simply a problem of emittance growth.

The old bunch spreader counts on the process of emittance growth sketched in figure 5. Figure 5a shows the 90% emittance contour of a bunch in phase space matched to the RF bucket. When the bunch spreader is gated on, the initial effect is to induce a bunch length (quadrupole) oscillation as shown in figure 5b. After a number of phase space oscillations (figure 5c), the emittance contour begins to deform due to the dependence of the synchrotron period on synchrotron oscillation amplitude. Finally, figure 5d shows the new 90% emittance contour after a large number of synchrotron periods. Note that the emittance of the bunch is indeed bigger, with a new bunch length approximately equal to the maximum bunch length during the height of the quadrupole oscillations.

This rate of emittance growth can be calculated by evaluating the growth in the synchrotron oscillation amplitudes of single protons. Based on a similar calculation in the transverse plane,⁴ the average amplitude increment per turn is

$$\frac{\Delta \langle I \rangle}{\langle I \rangle} = \left(\frac{\eta}{\Omega E} \right)^2 \frac{f}{8} \langle |k(2\Omega)|^2 \rangle \frac{\Delta \omega}{2\pi} \quad (3)$$

where I is the synchrotron oscillation amplitude in eV-sec and $\Delta I \ll I$, η is the momentum compaction, Ω is the particle angular synchrotron frequency in rad/sec, E is the beam energy in eV, f is the revolution frequency in Hz, $|k(2\Omega)|^2$ is the power per unit bandwidth of the bunch

4. S. Mane, private communication.

spreader induced longitudinal gradient variations, and $\Delta\omega$ is the bandwidth. Note that the growth in amplitude as a function of time will be exponential, where the growth rate is proportional to the square of the noise amplitude at twice the natural proton synchrotron frequency. If $\theta(t)$ is the RF phase variation introduced by the bunch spreader, ω_{rf} is the angular RF frequency in rad/sec, eV_{rf} is the peak rf energy gain per turn in eV, and ϕ_s is the synchronous phase angle, then

$$k(t) = \theta(t) \omega_{rf} eV_{rf} \sin(\phi_s) \quad . \quad (4)$$

For future reference, note that the RF voltage can be varied instead of the RF phase, so that

$$k(t) = \omega_{rf} eV_{rf}(t) \cos(\phi_s) \quad . \quad (5)$$

The dependence of the amplitude growth rate on the frequency content of the bunch spreader signal is very important. First, there is no growth in the amplitude of a proton by this mechanism unless some fraction of the spreader power spectrum is at twice the natural particle frequency. Second, there is a spread in the natural proton synchrotron frequencies for a finite length bunch. The functional dependence of the synchrotron period on oscillation amplitude is quite complicated, requiring evaluation of elliptic integrals.⁵ For phase oscillation amplitudes ϕ about the synchronous phase angle ϕ_s which are at most half of the distance between the unstable fixed point and synchronous phases, this functional dependence can be approximated by the relationship

$$\Omega(\phi) = \Omega(0) \left[1 - \alpha^2(\phi_s) \phi^2 \right] \quad , \quad (6)$$

where ϕ and ϕ_s are in degrees and

$$\alpha^2(\phi_s) = \beta_0 + \beta_2 \phi_s^2 + \beta_4 \phi_s^4 \quad (7)$$

$$\beta_0 = 0.194 \times 10^{-4} \quad \beta_2 = 0.194 \times 10^{-8} \quad \beta_4 = 0.603 \times 10^{-11} \quad .$$

5. G. Dome, "Theory of RF Acceleration and RF Noise", CERN Accelerator School Proceedings, Antiprotons for Colliding Beam Facilities, CERN 84-15, pg. 215 (December 20, 1984).

This approximation is best at zero synchronous angle,⁶ getting progressively worse as $\phi_s=90^\circ$ is approached. Figure 6 shows the calculated fractional synchrotron frequency deviations as a function of ϕ and ϕ_s , along with the fits which were compiled to generate the numerical values in equation 7.

Therefore, to excite emittance growth throughout the bunch, a sufficiently broad band spreader signal is required at twice the synchrotron frequency of the protons. While the later requirement was met in the old bunch spreader, the former was not.

Indeed, the theoretical response of the beam to the old bunch spreader is quite complicated. The differential equation describing the motion of a single proton with the natural synchrotron angular frequency ω_0 under the influence of a voltage gradient modulation near twice this natural frequency of amplitude a can be written as

$$\ddot{x} + \omega_0^2 [1 + a \cos(2\omega_a t)] x = 0 \quad . \quad (8)$$

The analytic solutions of this equation are called Mathieu functions.⁷ This solution is very complicated, with unexpectedly strong responses for particles where $\omega_a = \omega_0$. Therefore, this equation was simulated numerically.

The iteration time interval $\Delta\tau$ was chosen such that the natural tune of the oscillation was $\nu_0=0.005$, where

$$\omega_0 = 2\pi \nu_0 / \Delta\tau \quad . \quad (9)$$

Figure 7 contains two examples of the oscillations induced by the frequency modulation in equation 8. In figure 7a the tune difference is large enough that the particle oscillation is bounded, and the oscillation is simply amplitude modulated. In figure 7b the tune difference is small enough that the oscillation grows exponentially. Figure 8 contains power spectra for a number of tune differences. As the natural-modulation tune

6. S. Ohnuma, "The Bucket and the Beam", TM-1381 (January 22, 1986).

7. M. Abramowitz and I. Stegun, Handbook of Mathematical Functions, Dover Publications, Inc., New York (1972), pg.721.

difference decreases, the two frequencies creating the modulated amplitude waveform (like that in figure 7a) merge, and the amplitude begins growing exponentially with time. This exponentially growing motion is oscillating at the drive frequency, and for the choice of $a=10\%$ modulation, with a proton response bandwidth of roughly 2%. According to figure 6, at typical values of $\phi_s=60^\circ$ and rms bunch length of 25° , 50% of the protons fall within a bandwidth of 8%. Therefore, the observed coherent quadrupole oscillation signal is due to a small percentage (roughly 10%) of the particles in the proton beam achieving exponentially large synchrotron amplitudes.

A multiparticle simulation was written to investigate the response of an entire bunch to the spreader induced modulation. Figure 9 shows the longitudinal emittance as a function of time for both voltage and phase modulation. Though a quadrupole oscillation is definitely induced (but not shown), the emittance remains invariant. Looking at the results in figure 8, the reason for this phenomenon is clear. Since all the protons which are within the exponential response bandwidth of the modulation are oscillating at the drive frequency, no emittance growth due to tune spread is possible. The phases of all protons with exponentially growing amplitudes are identical throughout the duration of the bunch spreader gate. Only if the spreader modulation is shut off discontinuously can emittance growth take place.

The logical fix to this problem is to substitute the single frequency generated from the beam by a broad band noise source. Then all particles respond at their natural frequencies, and emittance growth due to tune spread is unimpeded. Figure 10 shows the longitudinal emittance for both voltage and phase noise modulation. The growth rate is clearly visible, and predictable using equation 3. Therefore, the design of a new bunch spreader was centered around the use of a broad band noise source.

Finally, the bunch spreader can be connected to a RF phase shifter (as is the case with the old bunch spreader) or to the RF peak voltage control (called the anode program, or APG). The problem with phase modulation is the need to decrease the radial offset feedback gain. In the case of RF voltage modulation and full gain, voltage gain per turn is conserved and

the synchronous phase is modulated. As the voltage is decreased, the synchronous phase is increased toward 90° . Therefore, the small amplitude voltage gradient is reduced by both voltage decrease and the $\cos\phi_s$ dependence of the gradient on synchronous phase. Voltage modulation seems to be the theoretically best channel for introducing a bunch lengthening signal into the Main Ring RF system.

1987/1988 Fixed Target Run Bunch Spreader

Broad Bandpass Noise

The block diagram for the 1987/1988 fixed target run Main Ring bunch spreader is shown in figure 11. The unique portion of this module is the noise generator, which amplifies and filters the white noise across a resistor. The initial version of the generator used two 2-pole low pass and two 2-pole high pass filters in series to shape the power spectrum of the noise voltage (see figure 12). The center frequency was chosen to correspond to twice the synchrotron frequency of the beam at some stable point after transition. Figure 13 contains the momentum, RF voltage, and synchrotron frequency waveforms during Main Ring acceleration. Since the synchrotron frequency hovers around 250 Hz during most of the post-transition acceleration period, the center frequency of the noise band was chosen to be at 500 Hz. Figure 14 shows the resultant noise power spectrum.

The circuit diagram for the 53 MHz beam monitor section of the 1987/1988 spreader appears in figure 15. The output of a beam detector is passed through a narrow band 53 MHz filter, and the resultant waveform is connected to the input of this section. This 53 MHz signal is peak detected and filtered by two 500 Hz second order low pass filters. This filtered voltage is proportional to $I(53 \text{ MHz})$ in equation 1, and is called M:BPD in the Fermilab control system.

The gate generator portion of the 1987/1988 bunch spreader circuit is shown in figure 16. The two external signals used by the electronics are the start time pulse and the final BPD stop level. At the start time the

value of BPD is sampled. When the ratio of the active BPD signal to the original BPD voltage drops below a certain percentage (determined by the voltage on the stop level input), the bunch spreader is gated off. If this trigger does not occur, the gate is terminated automatically after a set time (via the potentiometer on the 555 chip). Due to beam loss difficulties (described below), the stop level portion of the circuit could not be used.

Finally, the filtered noise is attenuated via a computer generated amplitude control voltage. The gated result is then summed with the existing anode program (APG) voltage. Figure 17 contains the circuit diagram of this mixer section.

This spreader circuit was built and connected to the RF APG circuit. Figure 18 is a plot of the Main Ring momentum (M:IB), beam intensity (M:MRBEAM), RF voltage (M:RFSUM), and the 53 MHz component of the beam (M:BPD) over four cycles. The bunch spreader was gated on at 1.25 sec into the cycle, and lasted for 0.8 sec (this is clear by inspecting the RF voltage waveform). In that time period, if the bunch spreader is off, BPD should increase while the beam intensity remains constant. The 53 MHz component of the beam increases during acceleration due to adiabatic damping. With the bunch spreader on the longitudinal emittance of the beam is certainly increased, but at the expense of beam intensity. As in the case of the old bunch spreader, the bunch spreader amplitude had to be adjusted to maximize the longitudinal emittance growth without excessive beam loss. In addition, the cycle to cycle variations in the bunch length were still very large (the phenomenon which caused the old bunch spreader to be investigated in the first place).

Sharp Active Filtered Noise

Assume that the phase space density distribution of the beam is nonzero at the edge of the RF bucket. The only way to increase the emittance of the Gaussian portion of the beam without beam loss would be to take advantage of the dependence of synchrotron frequency with synchrotron oscillation amplitude, applying a spreader signal with no spectral power at the synchrotron frequencies of large amplitude protons.

Therefore, a second version of the bunch spreader noise generator section was built, where the second order low and high pass filters were replaced by a sharp active filter network (see figure 19).

The criterion for the sharpness of such a filter is contained within figure 6. For synchronous phase angles greater than 40° (which is typical), the fractional synchrotron frequency decrease at which the proton amplitude starts approaching the unstable fixed points is roughly 25%. Therefore, if the synchrotron frequency is 250 Hz, the frequencies of large amplitude particles would be less than 180 Hz.

Since the synchrotron frequency is not stationary (see figure 13), but ranges from 175 Hz to 300 Hz in the portion of the Main Ring cycle of interest, the noise amplitude must encompass the range of frequencies from 350 Hz to 600 Hz. Using the criterion above, if twice the synchrotron frequency is 600 Hz, the minimum frequency of the bunch spreader signal should be 300 Hz. The amplitude growth rate is proportional to the square of the noise voltage. Assume that the maximum allowable growth rate of large amplitude particles is 1/1000 times the growth rate of small amplitude particle. Then the filter requirements are a lower 3db point of 350 Hz, with a amplitude reduction of 30 db by 300 Hz. Figure 20 shows the measured response of the active filter network in figure 19. The lowest peak is at 350 Hz, and the cursor is at 300 Hz, where the noise amplitude is 30 db less than the amplitude of the 300 Hz peak.

This version of the bunch spreader was placed into the Main Ring RF system and tested. First, the beam intensity losses were dramatically reduced, though not eliminated. Figure 21 shows the bunch length at Main Ring flattop with and without the bunch spreader, clearly showing the growth in emittance induced by the applied noise. Figure 22 shows the corresponding BPD and RF voltage curves. Note that the gate width was reduced to 1/2 second. This was done because beam intensity losses were sensitive to the starting time of the spreader gate, indicating that certain synchrotron frequencies were particularly sensitive. Reducing the gate width and adjusting the starting time decreased beam losses to negligible levels (less than 1%).

The final state of the bunch spreaders in the Main Ring has two modules which are independently timed and contain noise spectra matched to their optimized starting times. The first module is described above. The second module has a one second gate width and a lower and narrower frequency band. They are used in tandem to maximize the final longitudinal bunch emittance while minimizing beam losses (which get worse as the beam intensity of the Main Ring increases).

Proposed Future Bunch Spreader

Work is presently underway to design and build more efficient bunch spreaders for the Main Ring and the Tevatron. The goal is to produce longitudinal growth with less beam loss than the present bunch spreaders. After studying the performance of the present spreaders, along with the theory of stimulated beam response and Mathieu functions, it is possible that smaller noise amplitudes applied over longer periods of time is the approach to take.

Figure 13 shows the variation of synchrotron frequency during the ramp. Of interest is the region between transition crossing and flattop. Figure 23 is a similar plot for the Tevatron, also showing synchrotron frequency as a function of time. Since there is no transition crossing in the Tevatron, the entire ramp period is available for bunch spreading. Clearly, the new bunch spreaders in both accelerators should have time dependent noise frequency capability.

In figure 14 there are two specific times at which beam loss takes place. The first is at transition, is not relevant to this discussion. The second, around 1.7 seconds, occurs in the middle of the bunch spreader activation period. Since beam loss is time dependent, it should be advantageous to have a time dependent noise amplitude curve.

A major difference between the Main Ring and Tevatron RF systems is the lack of frequency or phase feedback on the Tevatron beam. Since the physics of emittance growth due to phase noise at the synchrotron frequency is well understood, lacking the nonlinear effects seen in the

Mathieu functions, the new Tevatron bunch spreader should try this dipole phase oscillation/noise approach.

Finally, the instabilities in the Tevatron which are largely responsible for the necessity of bunch spreading are proving to be quite difficult to identify and correct. One problem in the work to diagnose these instabilities is the ramp to ramp variations in beam intensity and bunch length. A computer program should be written which controls the amplitude of the Tevatron bunch spreader in a feedback type manner. Depending on whether the user requests consistent bunch length or peak current (beam intensity divided by the bunch length), the program adjusts the noise amplitude so that the quantity of interest is reproducible on a ramp by ramp basis.

Conclusions

The performance of the past Main Ring bunch spreader has been reviewed and analyzed. On the basis of this work, it was concluded during the 1987/1988 fixed target run that a new bunch spreader utilizing random noise was required. Two versions of this new hardware were tested, both inducing more stable and effective longitudinal emittance growth. Comparing the performance of the two modules, one with a broad noise source and the other with sharply delimited noise bandwidth, it was clear that beam loss was related to the noise power at frequencies coincident with two times the synchrotron frequency of large amplitude particles.

In the future, variable noise frequency and amplitude will be implemented, with the hope that beam loss can be further minimized. In addition, a new Tevatron bunch spreader will also be contemplated.

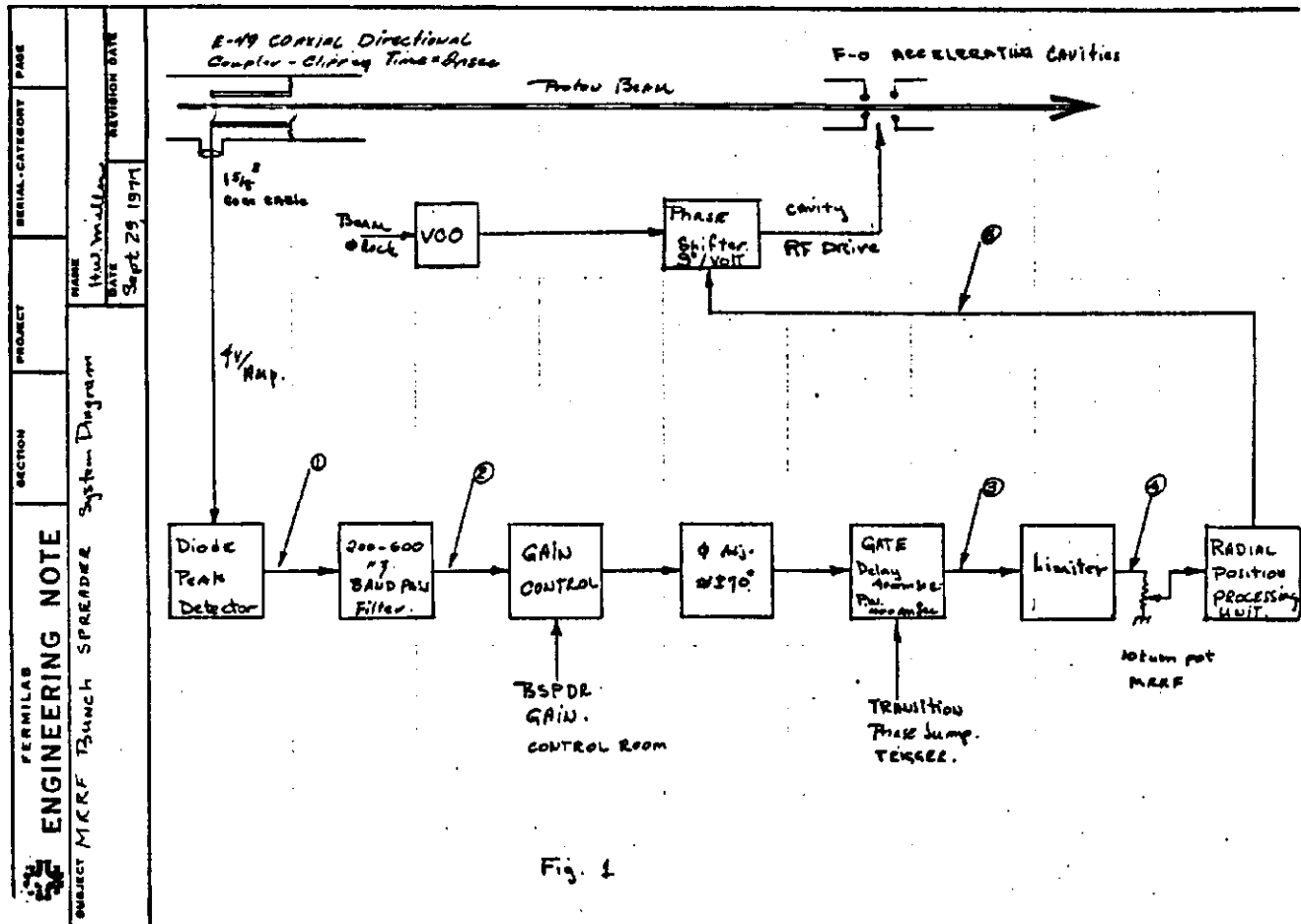
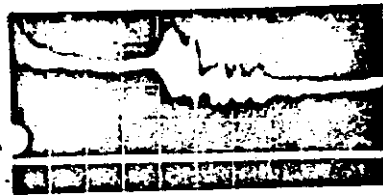


Figure 1: Reproduction of figure 1 in the appendix of EXP-86, containing a block diagram of the old Main Ring bunch spreader electronics.



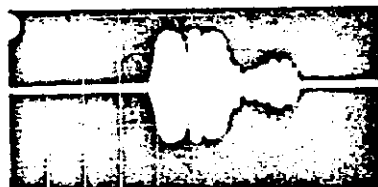
1. Diode Peak Detector
Vert: 2V/div.



2. BSPDR 400 Hz Filter
Vert: 1V/div.



3. BSPDR Output
Vert: 1V/div.



4. BSPDR Limit
Vert: 0.5V/div.



5. Phase Shifter Drive
Vert: 0.2V/div.
Signal Band Width 200-400 Hz.

TYPICAL BUNCH SPREADER SIGNALS

$I = 1.6 \times 10^{13}$ ppp; BSPDR:GAIN = 0.88; Limit = 0.60
Scope Trigger = Transistion, Sweep - 100 msec/div.

Fig. 2

Figure 2: Reproduction of figure 2 in the appendix of EXP-86, containing sample waveforms at several test points in the old Main Ring bunch spreader electronics. The top photograph shows the output of the bunch peak detector, which in the absence of noise is inversely proportional to the bunch length and proportional to the bunch intensity.

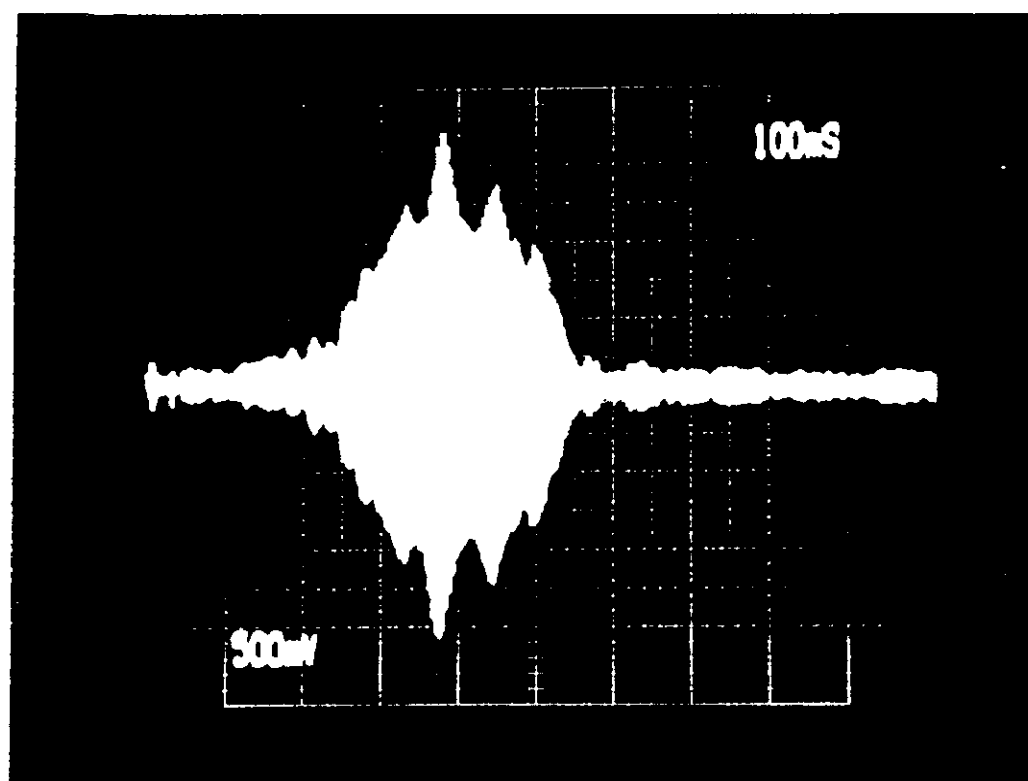


Figure 3: Present response of the 53 MHz component of the longitudinal bunch shape to the old bunch spreader. For fixed bunch intensity, the larger the signal the smaller the bunch length. Note that although quadrupole (bunch length) oscillations are excited, the DC level of the signal, and hence the longitudinal bunch emittance, is unaffected.

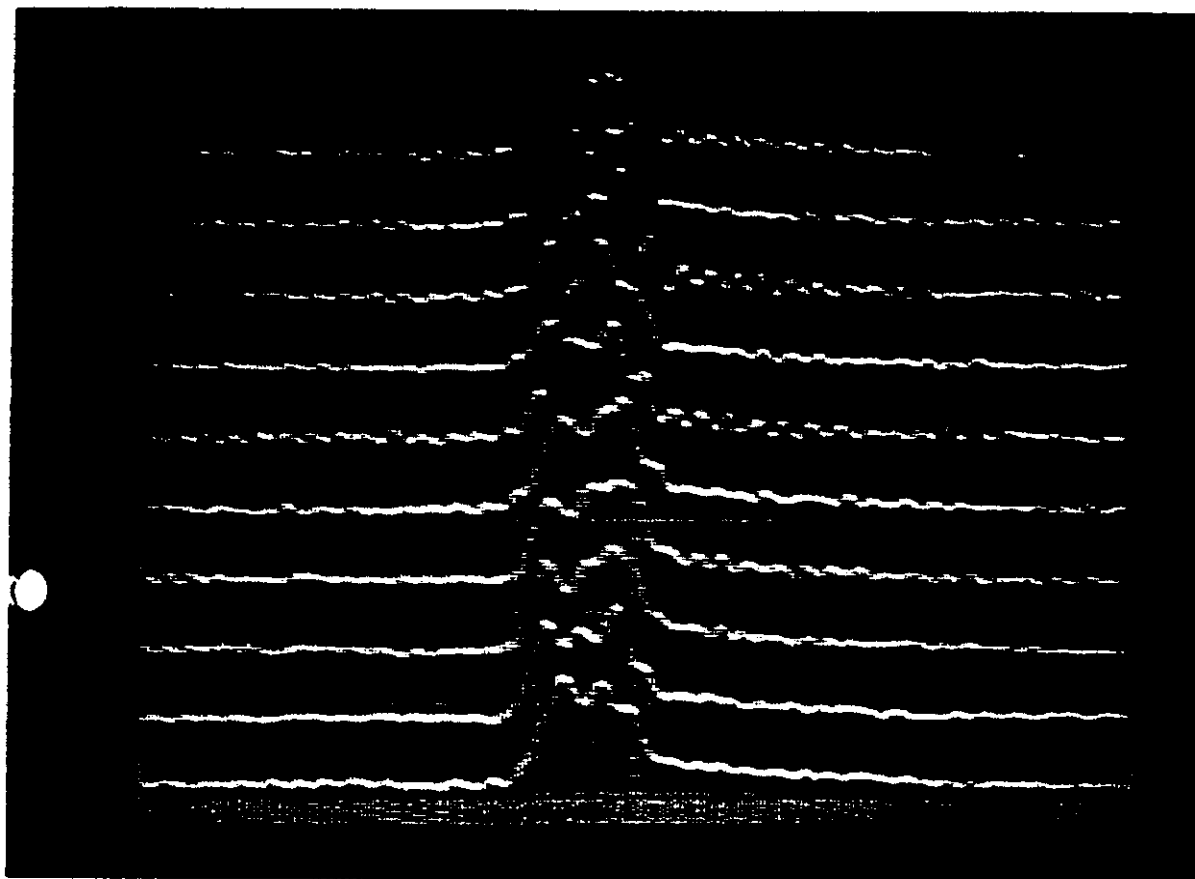


Figure 4: Sample mountain range display of a proton bunch during the time when the bunch spreader is normally on. Even though the full length of the bunch is not changing dramatically, the peak intensity of the bunch is varying significantly due to noise spikes. The scale is 2 nsec/div.

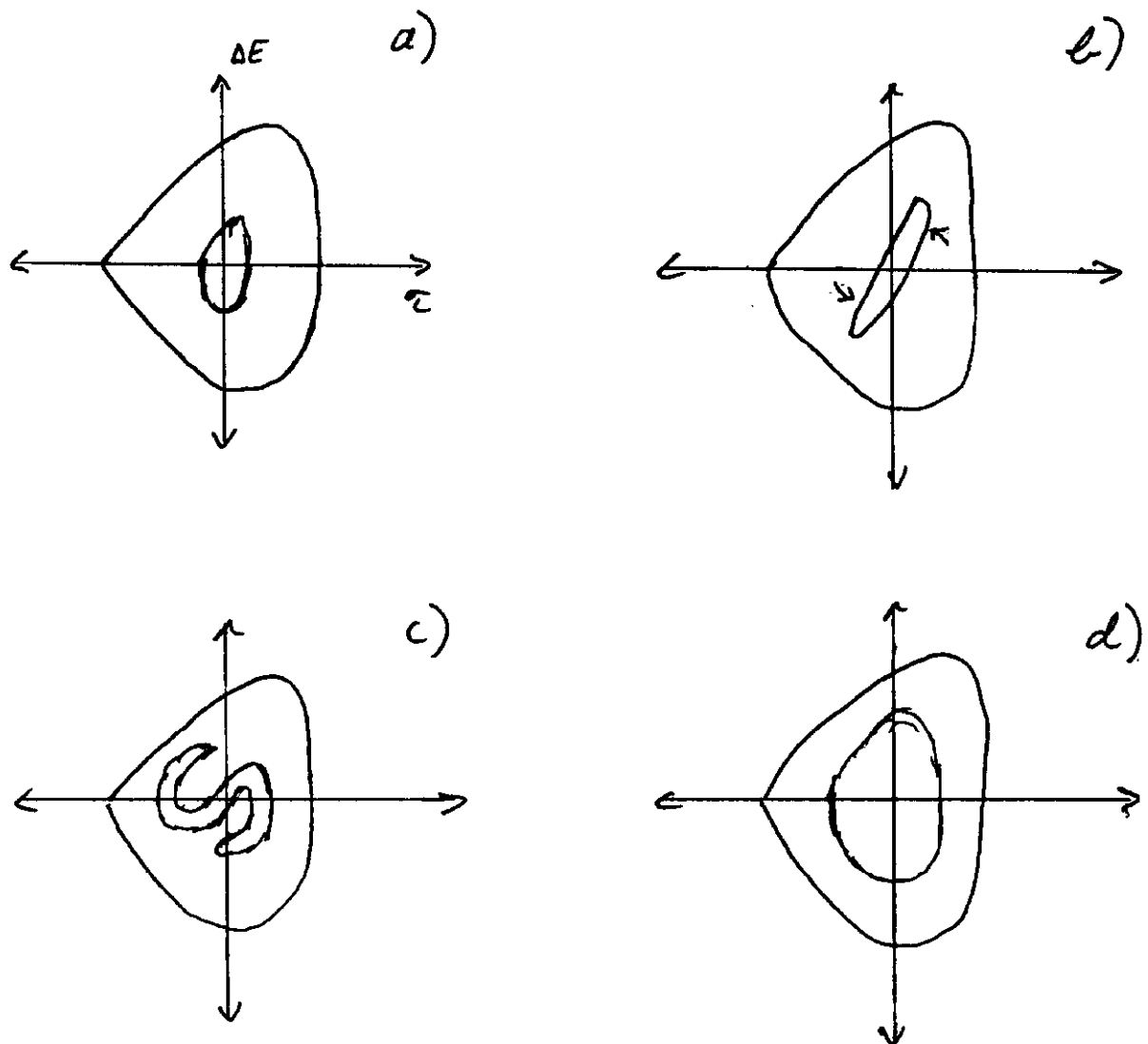


Figure 5: Expected stages of beam response for the old bunch spreader. At first (a) the bunch is matched to an accelerating RF bucket. Shortly after the bunch spreader is gated on (b) the quadrupole oscillations begin. After a number of synchrotron periods (c) the amplitude dependence of the oscillation frequency begins to smear out the bunch density distribution. Finally, after many synchrotron periods (d) the bunch is again matched to the accelerating RF bucket, but now has a larger phase space area, or emittance.

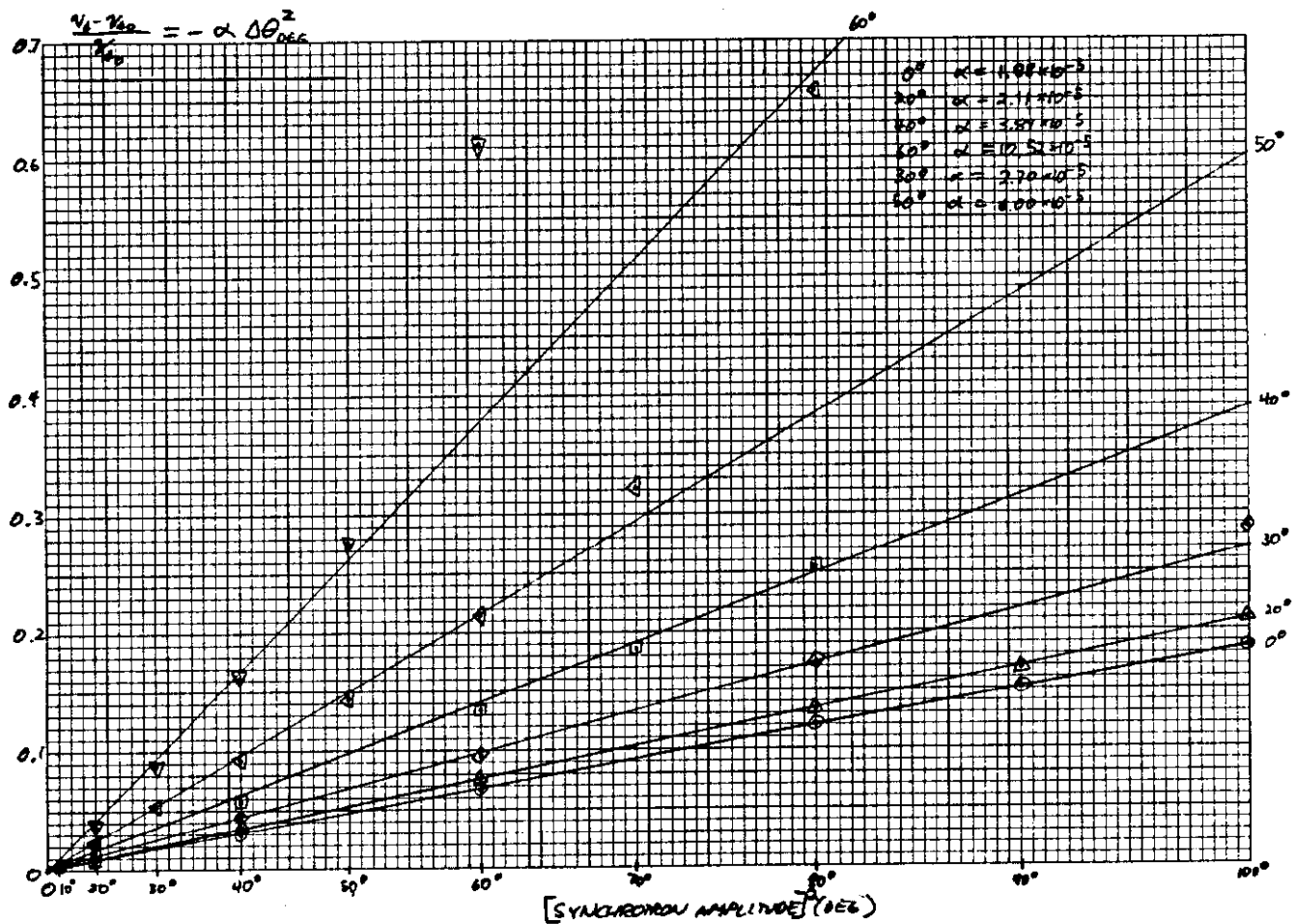


Figure 8: Calculation of the synchrotron frequency of a proton as a function of synchrotron amplitude and the synchronous phase of the oscillation. The lines are representative fits to the data over the region of phase amplitude normally occupied by Main Ring bunches.

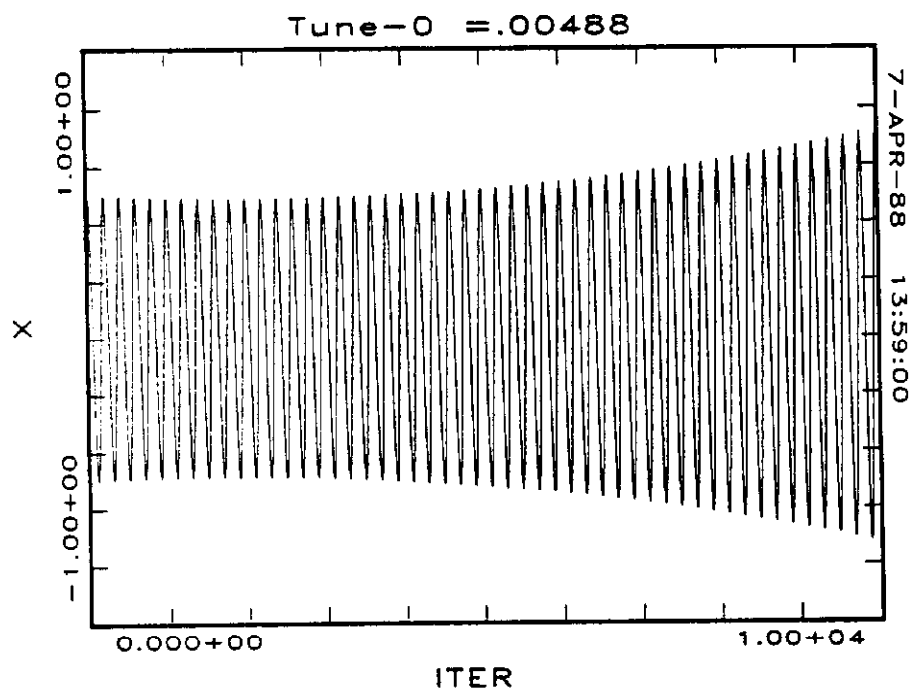
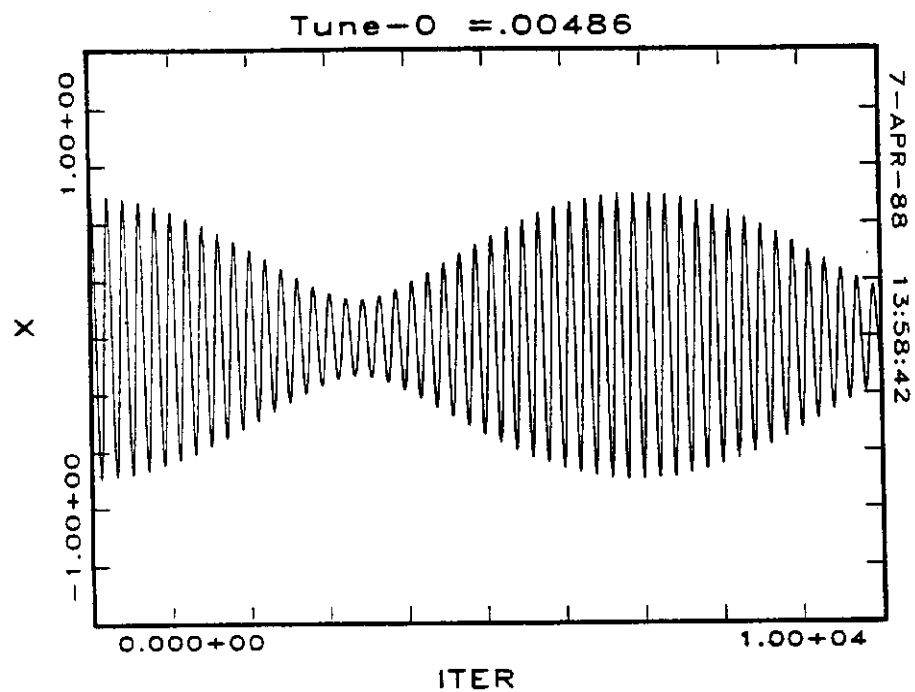


Figure 7: Simulation of the response of a single proton to a single frequency modulation of its natural frequency. In both plots the modulation tune is 0.005. In 7a the natural tune of the proton is 0.00486, and the motion is bounded with a simple sinusoidal amplitude modulation. In 7b the natural tune is 0.00488, small enough to cause the proton oscillation to lock onto the modulation tune. As a result, the amplitude of its oscillation grows exponentially.

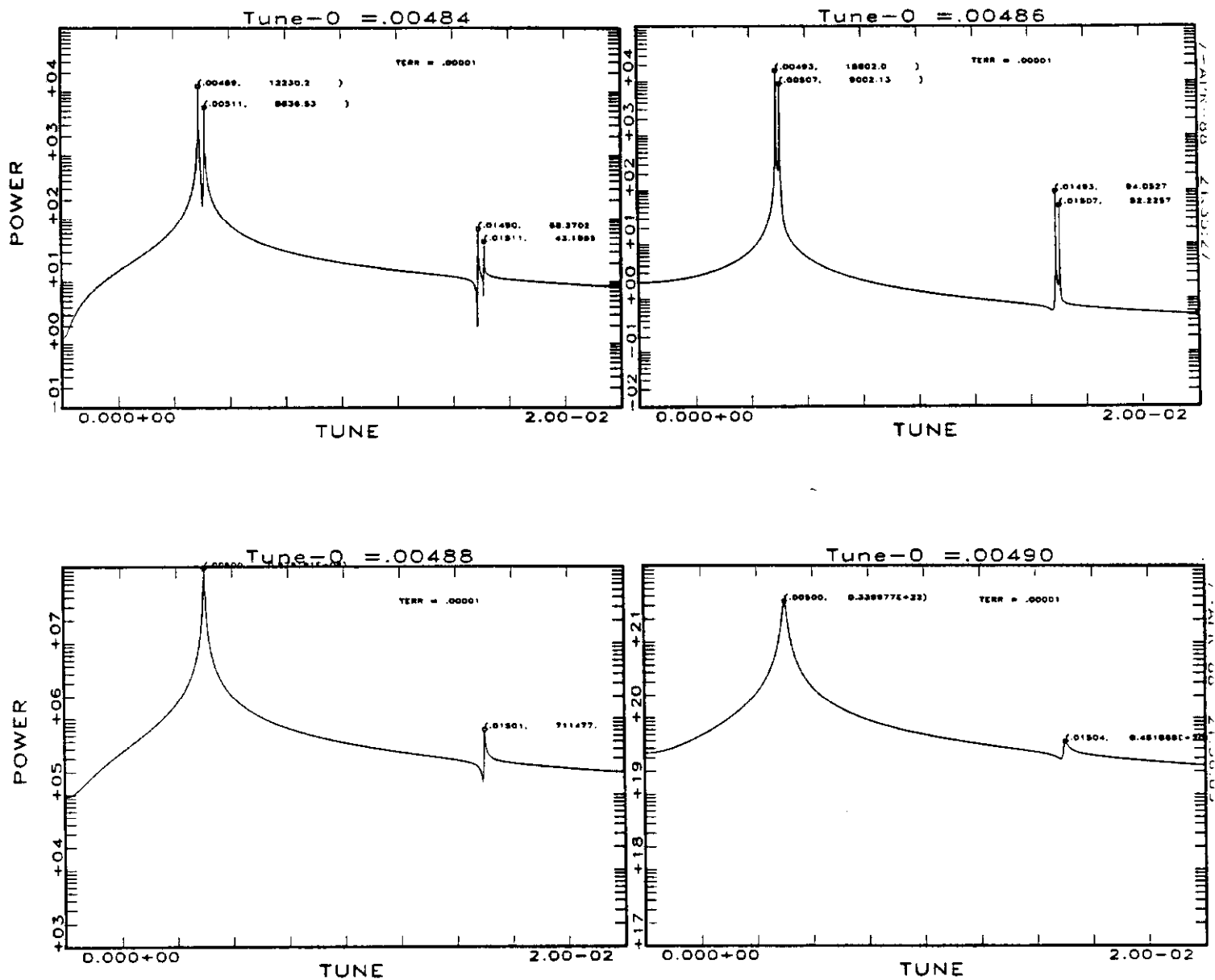


Figure 8: Fast fourier transforms of the two scenarios presented in figure 7, along with runs with both larger and smaller tune differences. In the cases with large tune differences, the motion corresponds to figure 7a, where the two tune lines simply produce the amplitude modulation. In the cases with sufficiently small tune differences, only a single line appears, whose width (and hence the oscillation amplitude growth rate) increases as the tune difference decreases.

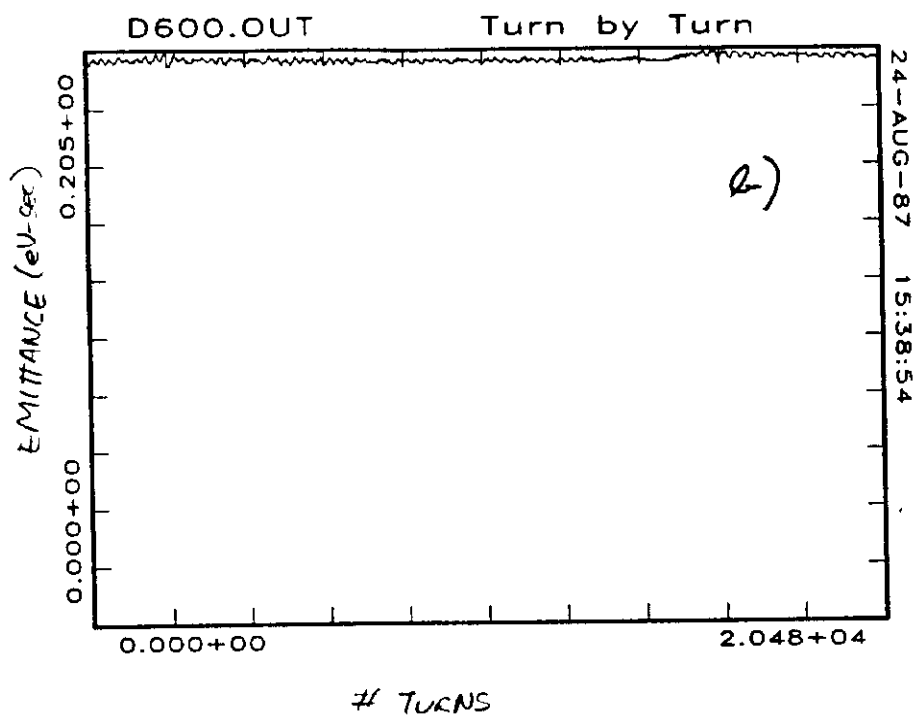
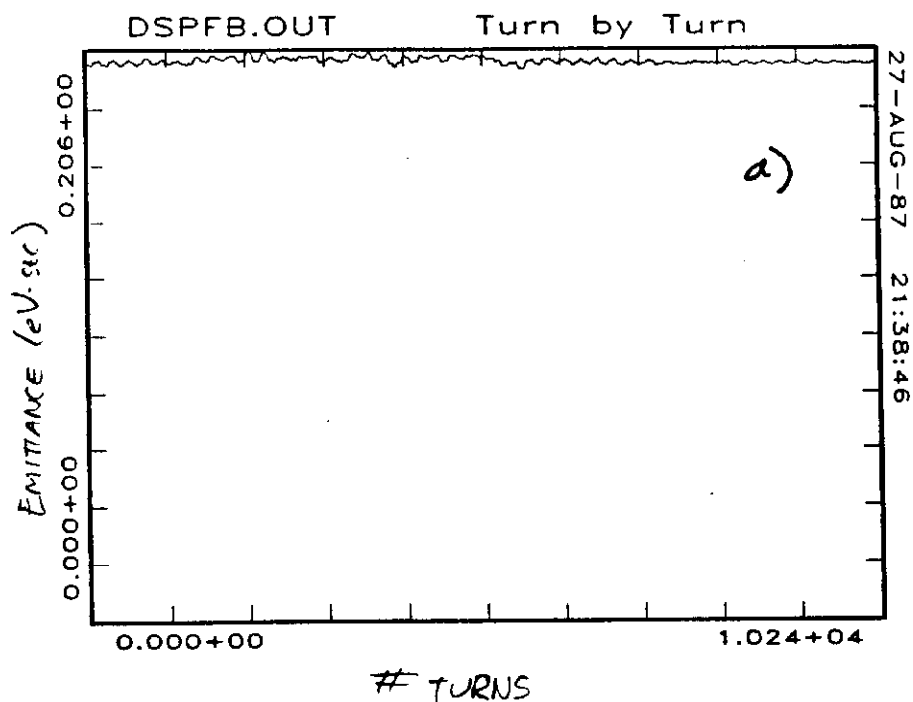


Figure 9: Numerical simulations of the response of a proton bunch to the old Main Ring bunch spreader, where the spreader signal is introduced as phase (a) or RF voltage (b) modulation. Note that no emittance growth is apparent.

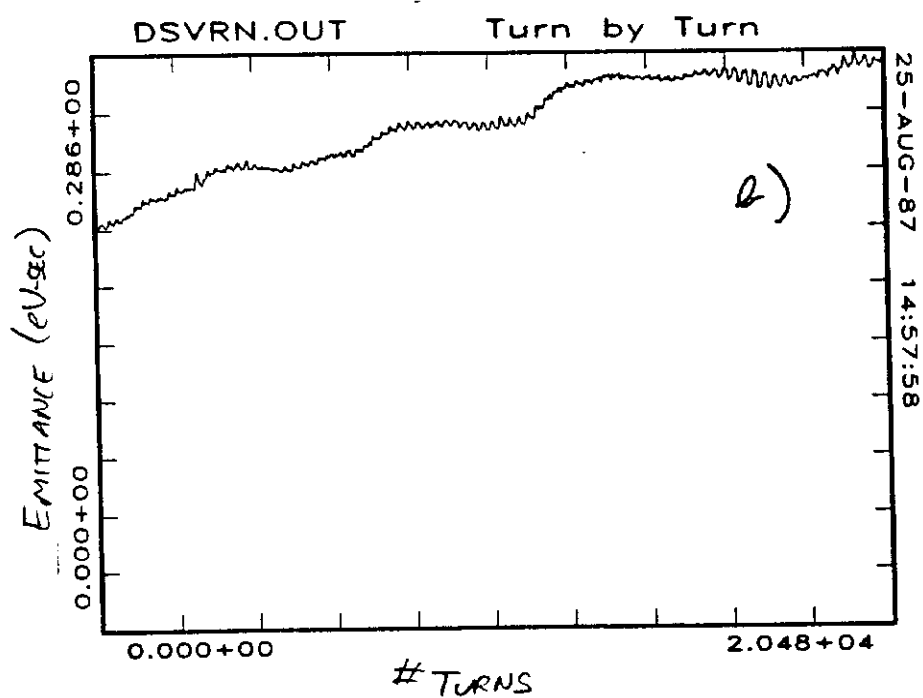
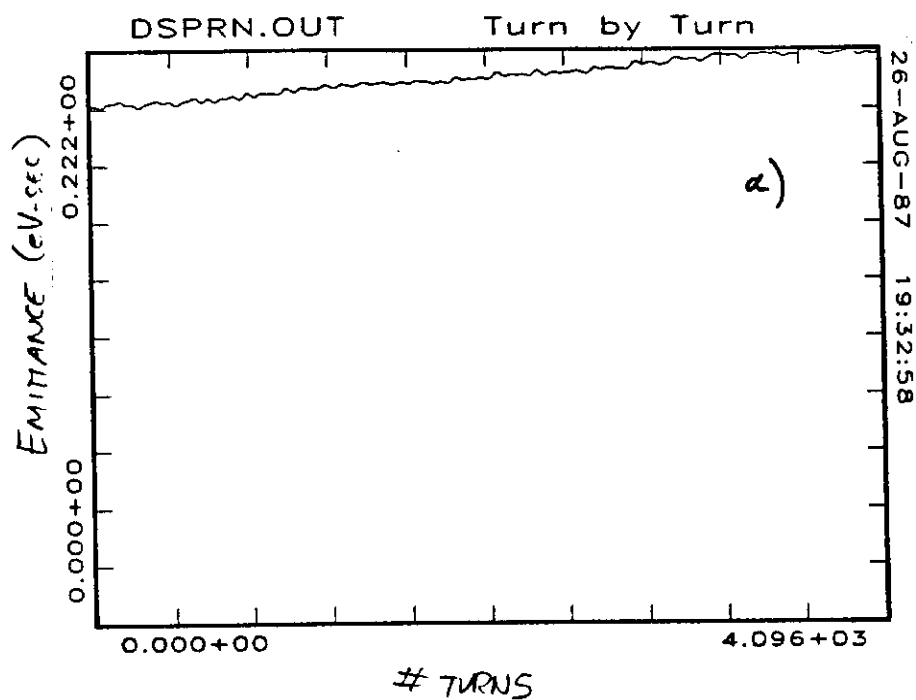


Figure 10: Numerical simulation of the response of a proton bunch to broad band noise, where the noise is introduced as phase (a) or RF voltage (b) modulation. In contrast to figure 9, emittance growth is clearly visible.

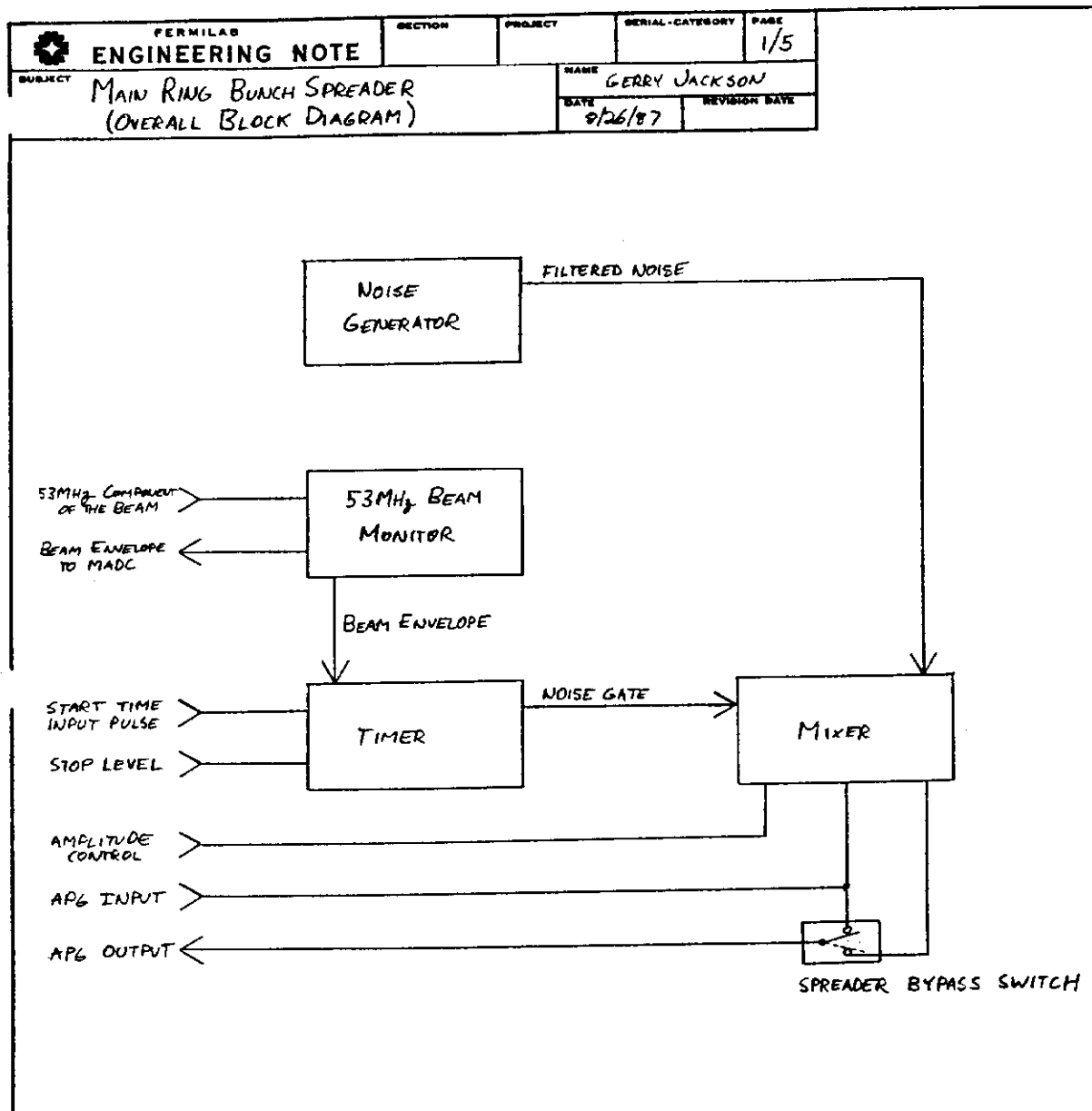


Figure 11: Block diagram of the 1987/1988 fixed target run Main Ring bunch spreader. A noise voltage is gated and mixed onto the RF voltage control signal, called M:APG in the Fermilab control system. The circuit can also be connected to the phase shifter portion of the Main Ring RF system. The beam envelope input to the noise gate was not used due to beam loss difficulties.

ENGINEERING NOTE MAIN RING BUNCH SPREADER (NOISE GENERATOR SECTION)	DESIGNER	REVIEWER	DATE
	NAME	DATE	REVISION
	GERRY JACKSON 7210	8/26/87	

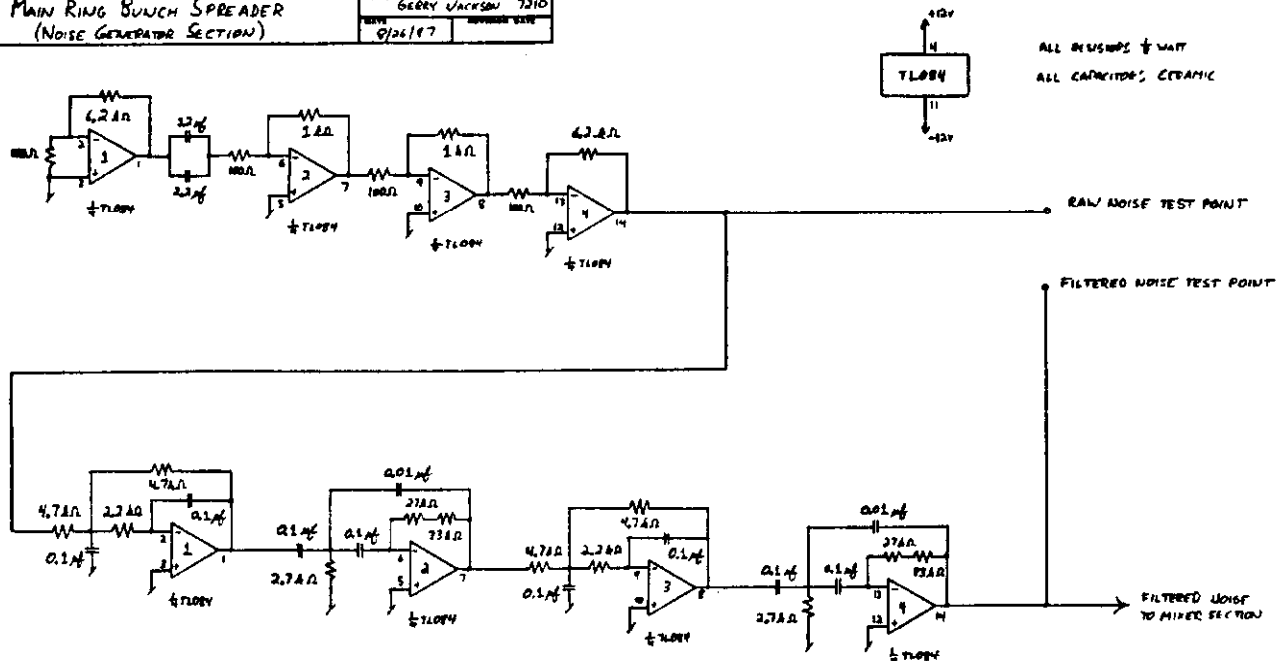


Figure 12: Circuit diagram of the first version of a noise generator for the 1987/1988 bunch spreader. It simply amplifies the thermal noise spectrum of a resistor, and then filter that signal through a series of second order low and high pass filters.

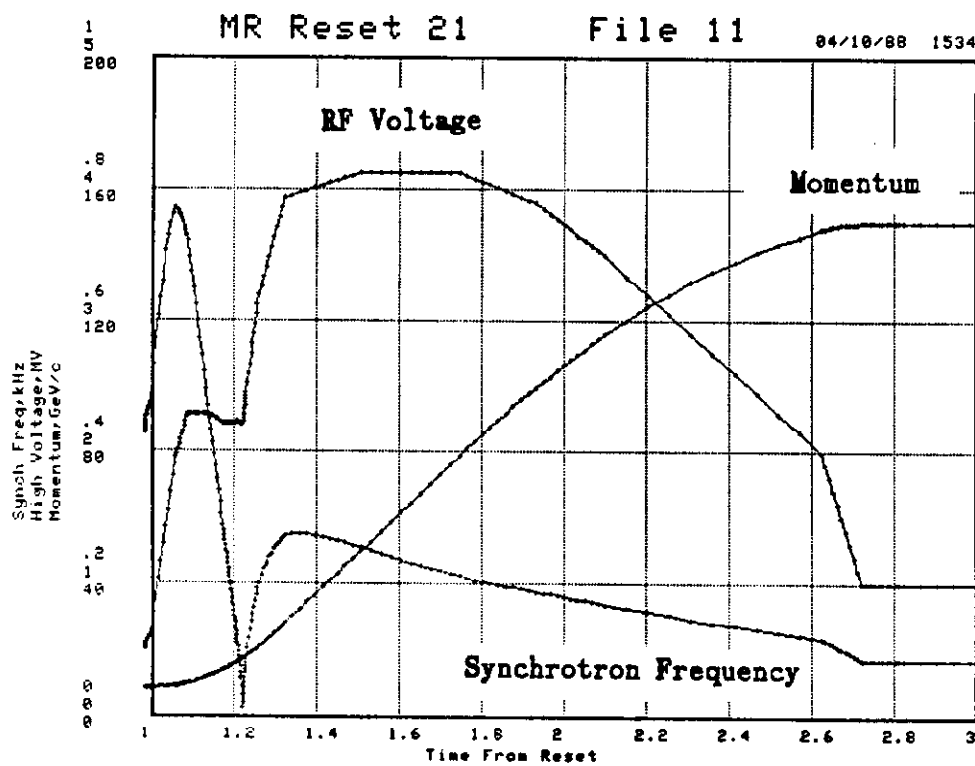


Figure 13: Plot of the Main Ring RF voltage, beam momentum, and small amplitude synchrotron amplitude during acceleration. At transition the synchrotron frequency dips to zero, after which it peaks up to approximately 300 Hz and then decays to 100 Hz.

Y=-34.497 dBVrms

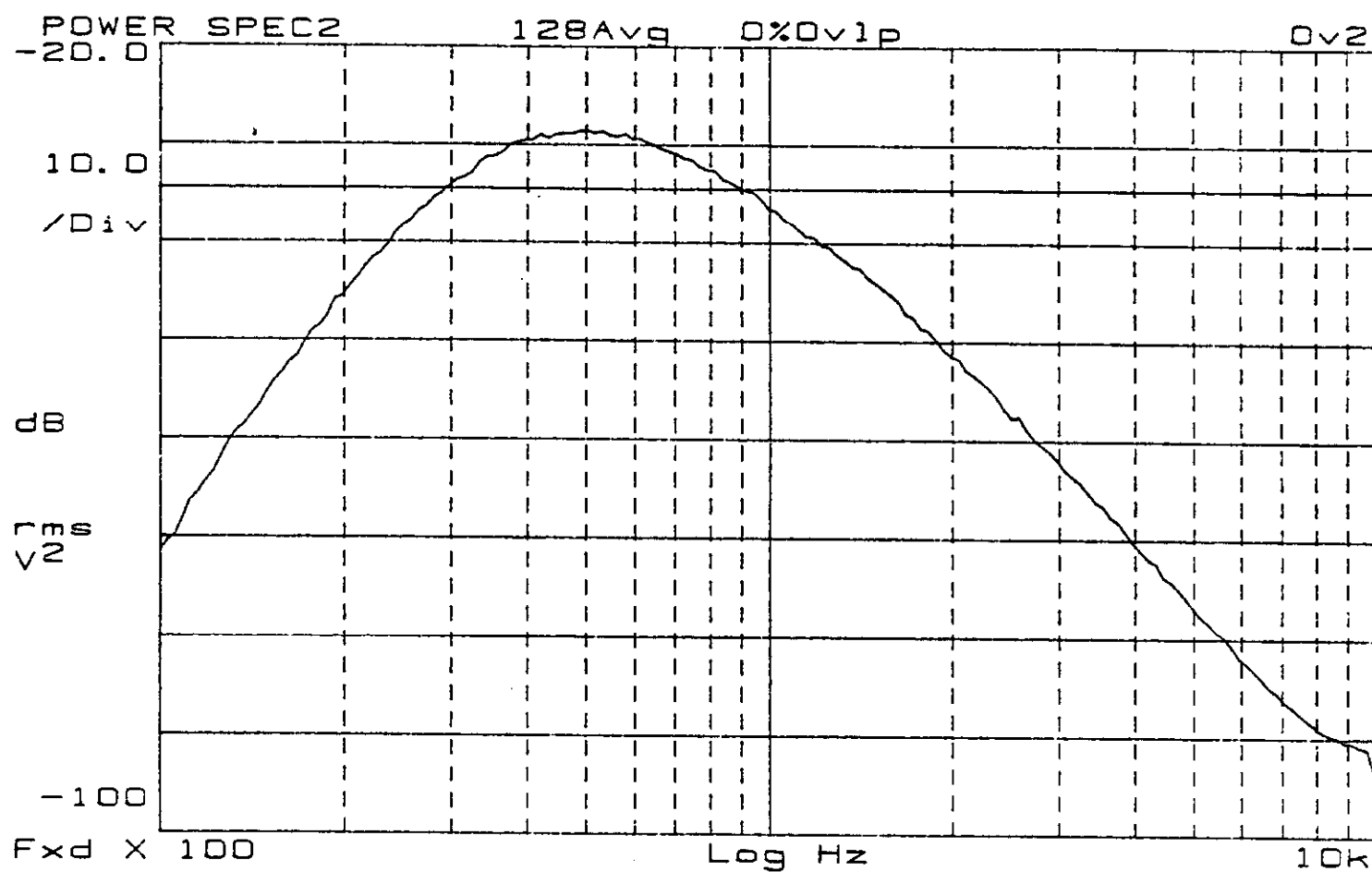


Figure 14: Initial noise spectrum injected into the Main Ring RF system. The peak of the bandpass is at 500 Hz (roughly twice the peak synchrotron frequency) and rolls off to either side at 80 db/decade.

PERMILAR	ENGINEERING NOTE	DESIGN	PROJECT	SERIAL CATEGORY	PAGE
PROJECT	MAIN RING BUNCH SPREADER (53MHz BEAM MONITOR SECTION)	NAME	GERRY JACKSON	DATE	8/26/87
		REVISION			

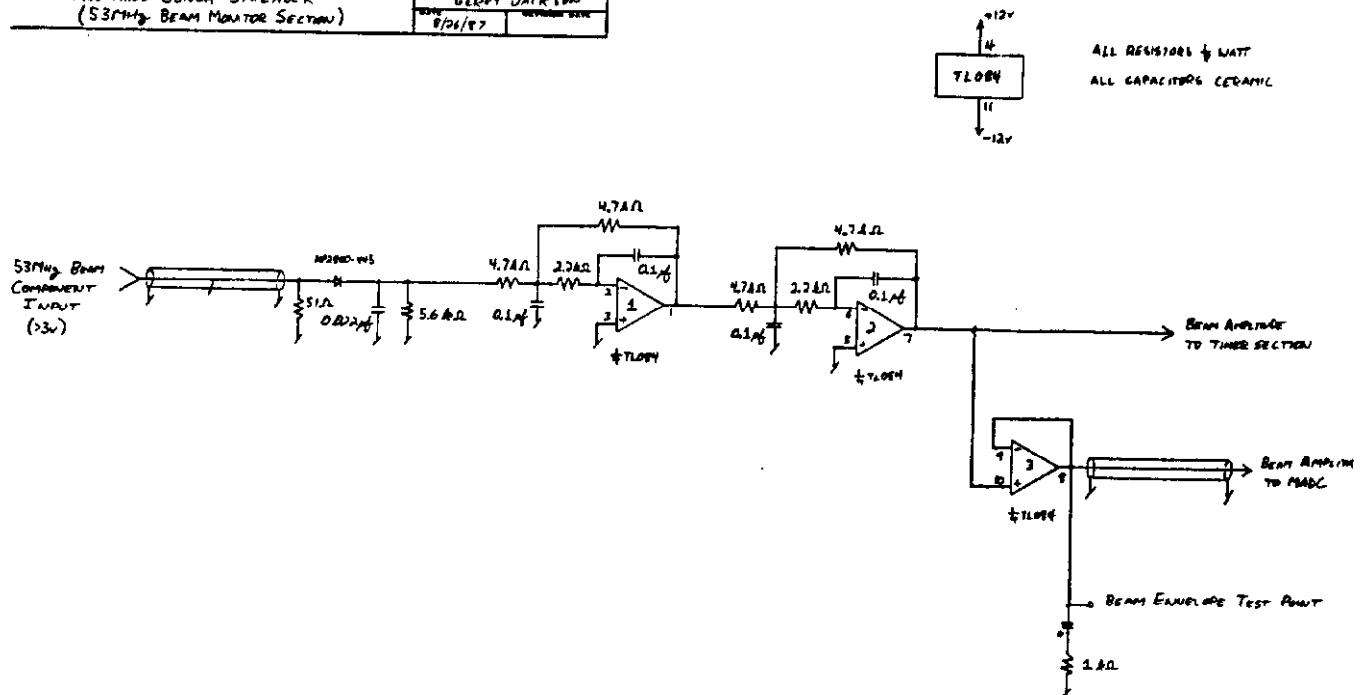



Figure 15: Circuit diagram of the 53 MHz beam component monitor section of the 1987/1988 bunch spreader. The 47.7 kHz revolution harmonics in the resultant peak detected voltage are filtered out by the two second order low pass filters.

Figure 16: Gate section circuit diagram of the 1987/1988 bunch spreader. The gate is terminated either by a sufficient drop in BPD or by a set time delay, whichever comes first. The BPD portion of the gate was not used due to beam loss difficulties.

 ENGINEERING NOTE	SECTION	PROJECT	DATE	5/5
	MAIN RING BUNCH SPREADER (MIXER SECTION)			
	GERRY JACKSON			
	8/24/87			

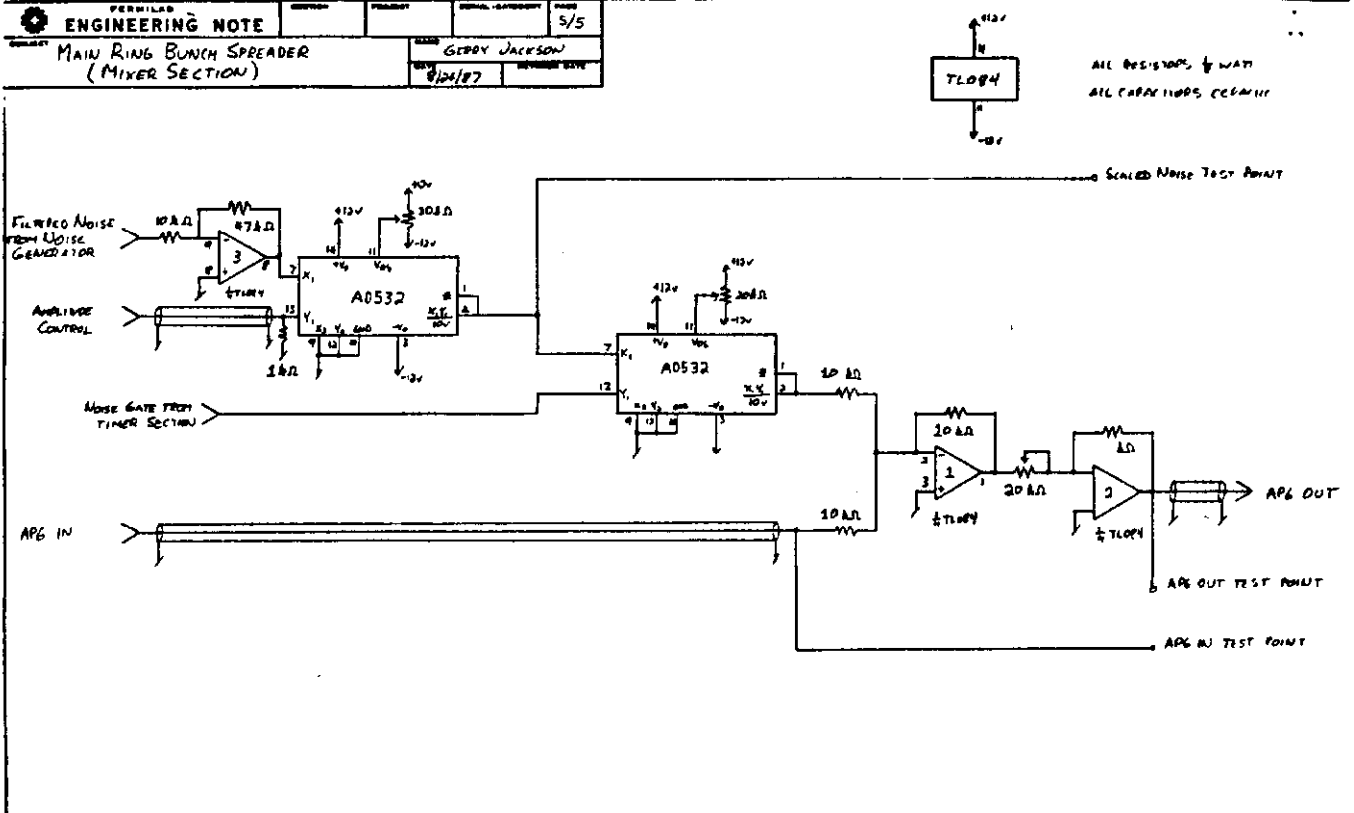


Figure 17: Circuit diagram of the mixer section of the module. The gate and amplitude modulation of the noise spectrum is imposed here, with the resultant voltage added to the RF voltage control (APG).

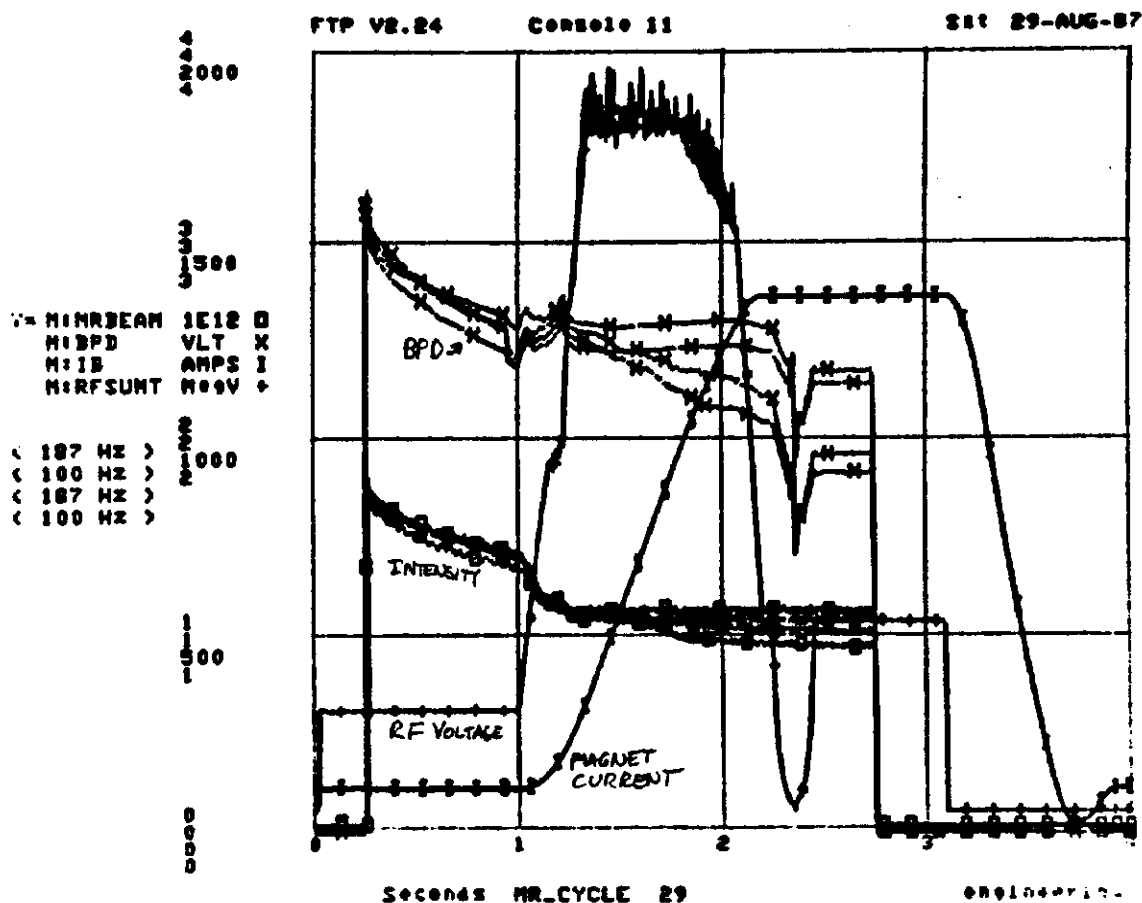


Figure 18: Typical behavior of the beam under the influence of the first version of the 1987/1988 bunch spreader. Note that although bunch lengthening occurs (since BPD drops during the spreader gate), beam intensity losses also occur.

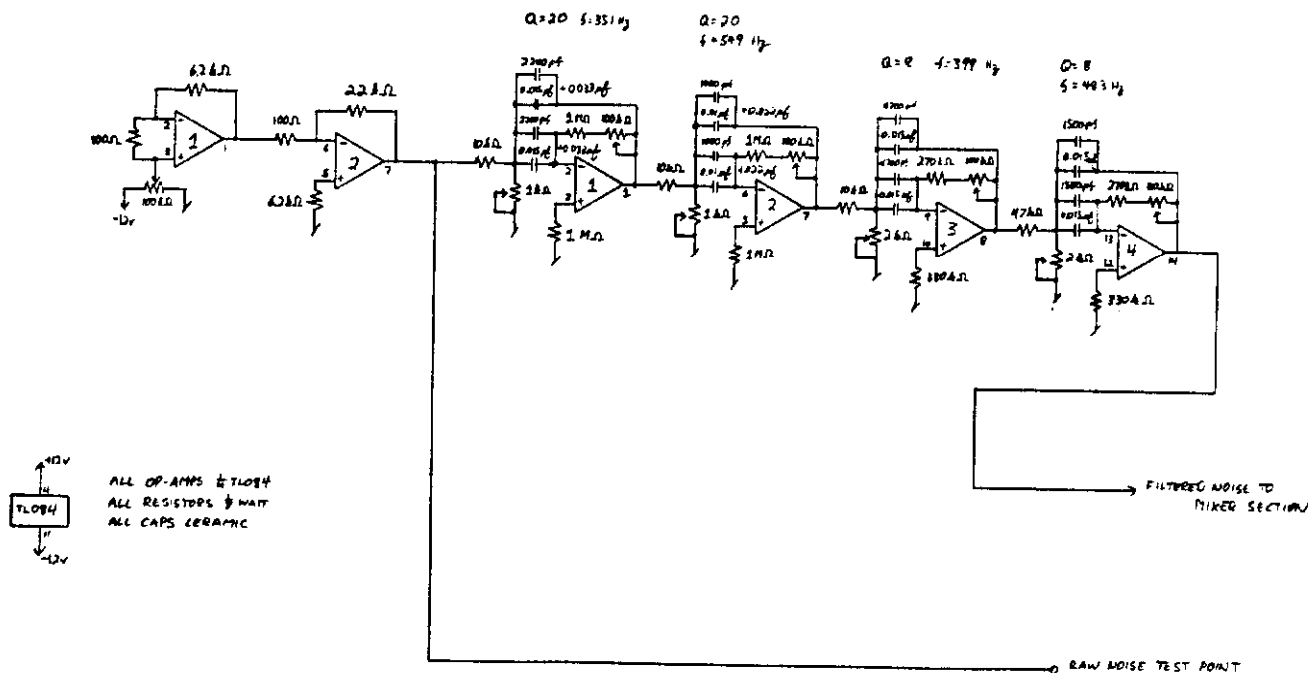


Figure 19: Circuit diagram of the second version of the noise generator of the 1987/1988 bunch spreader. The second order low and high pass filters have been replaced by an active filter bandpass network.

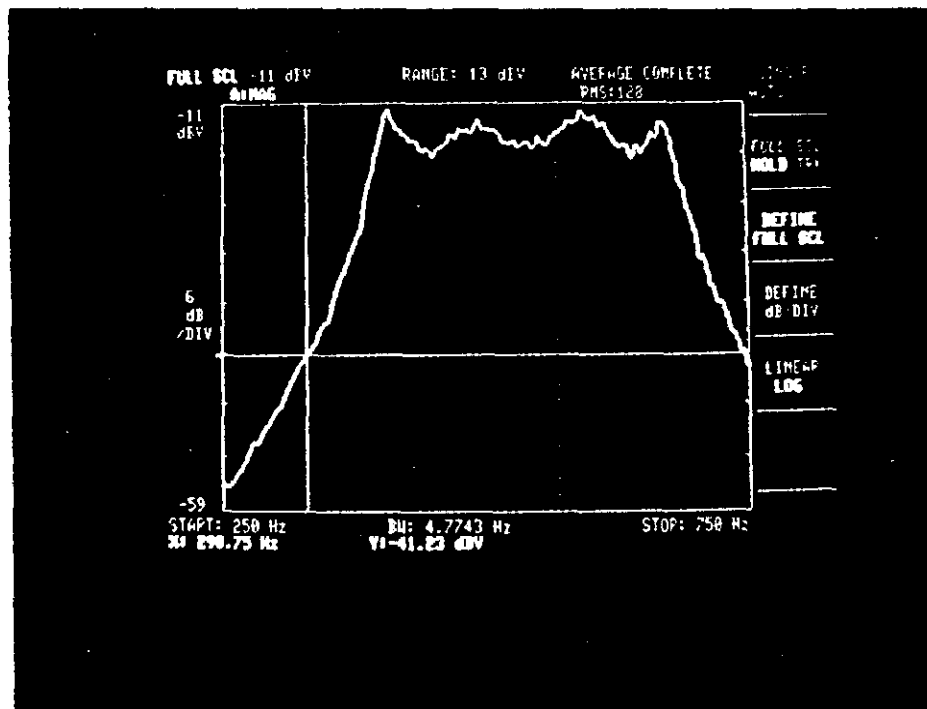


Figure 20: Noise spectrum generated by the second version of the noise generator of the 1987/1988 bunch spreader. The cursor is at 300 Hz, showing that in 50 Hz the noise dropped by 30 db, the design criteria for the circuit.

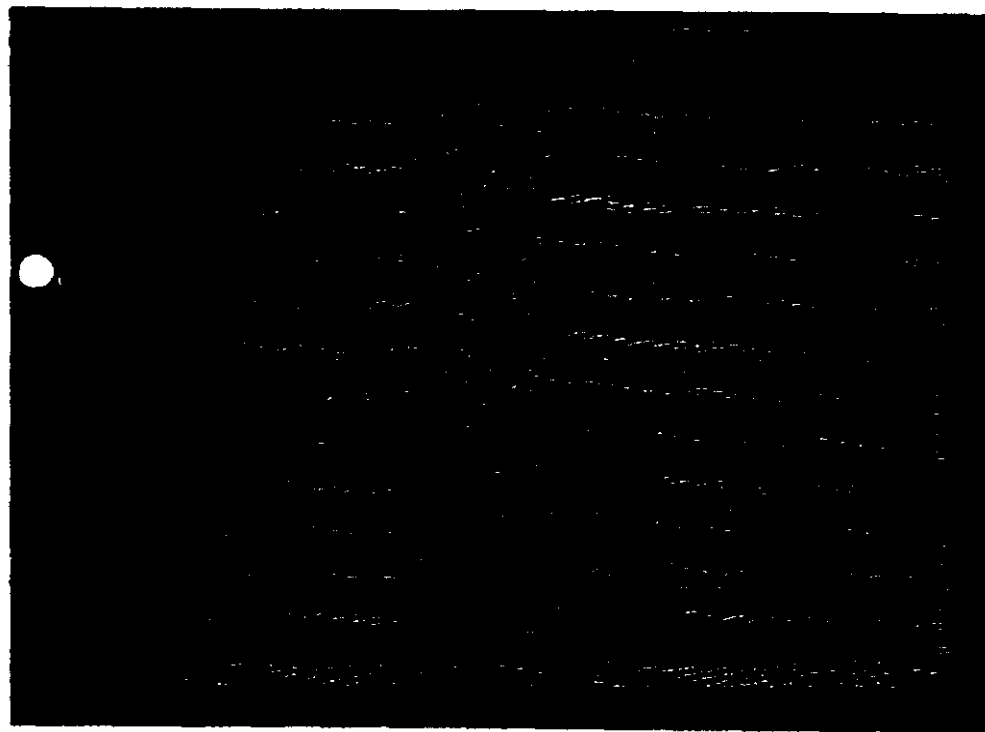
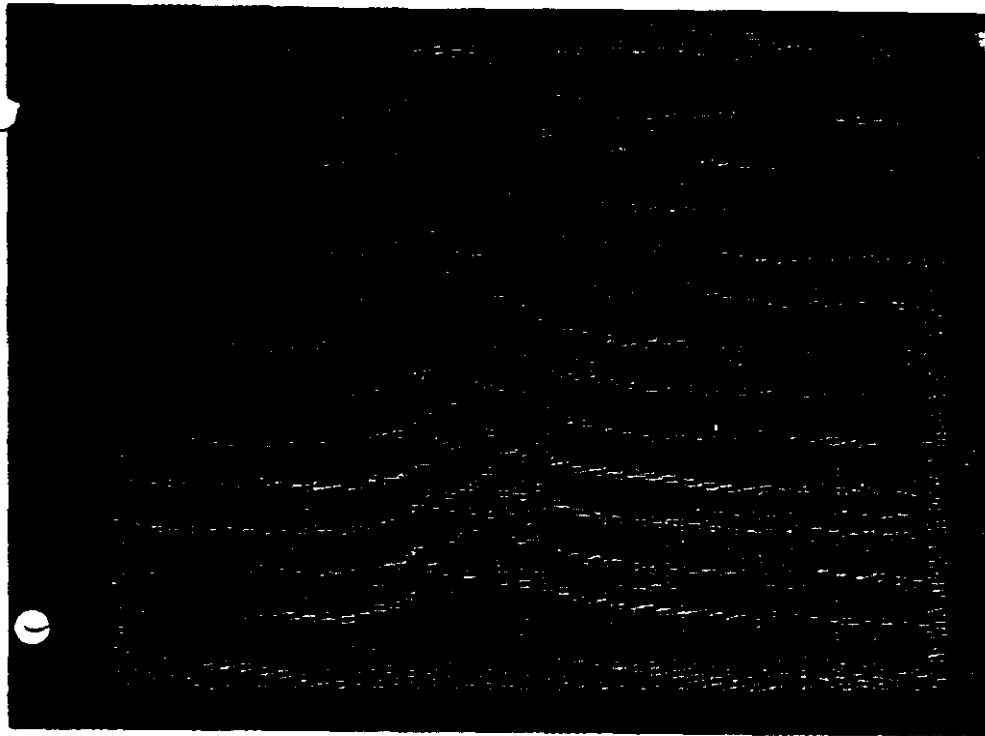


Figure 21: Longitudinal bunch profile (a) with and (b) without the second version of the 1987/1988 bunch spreader. The scale is 2 nsec/div.

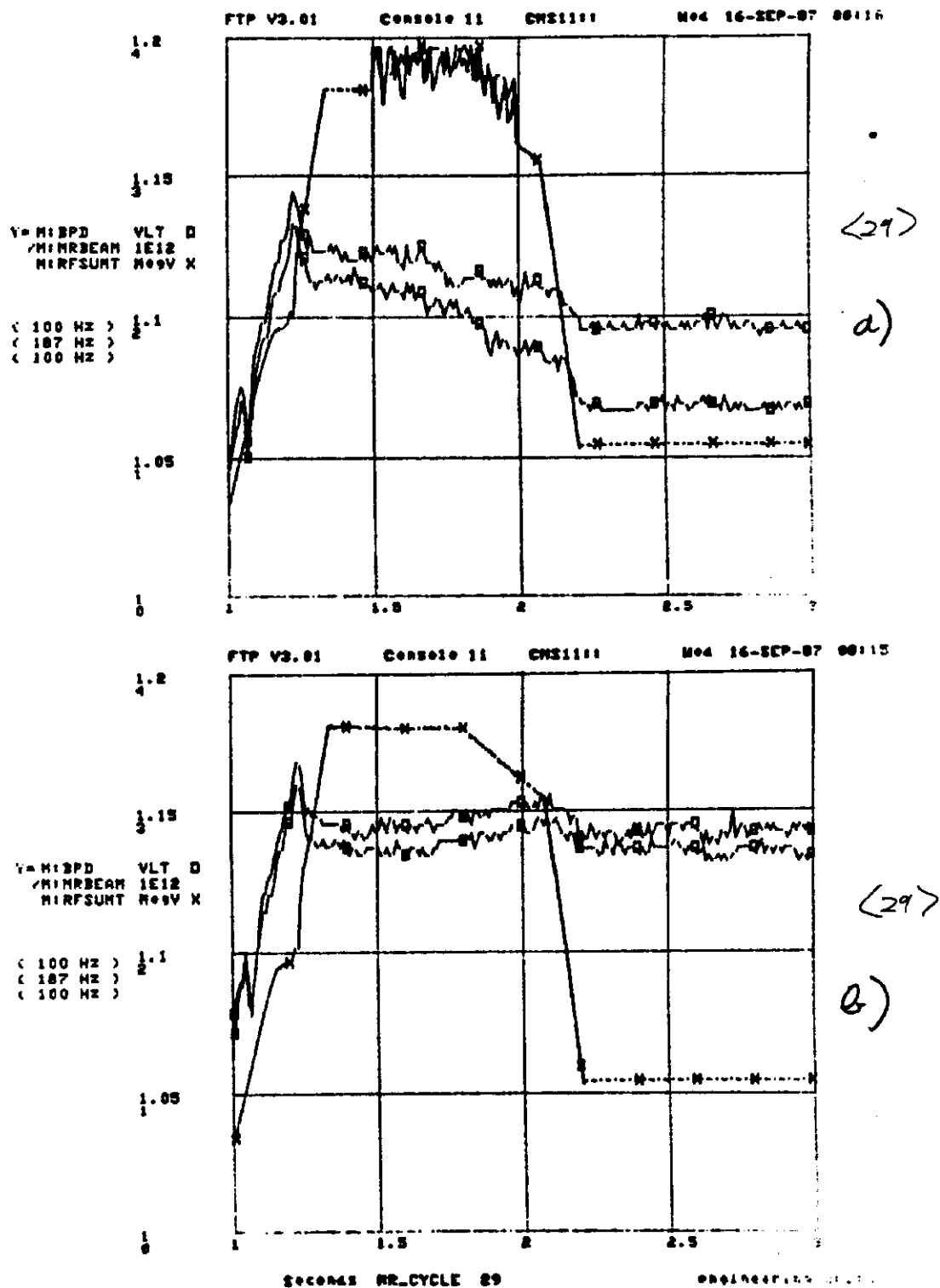


Figure 22: RF voltage and ratio of BPD to the beam intensity (a) with and (b) without the second version of the 1987/1988 bunch spreader.

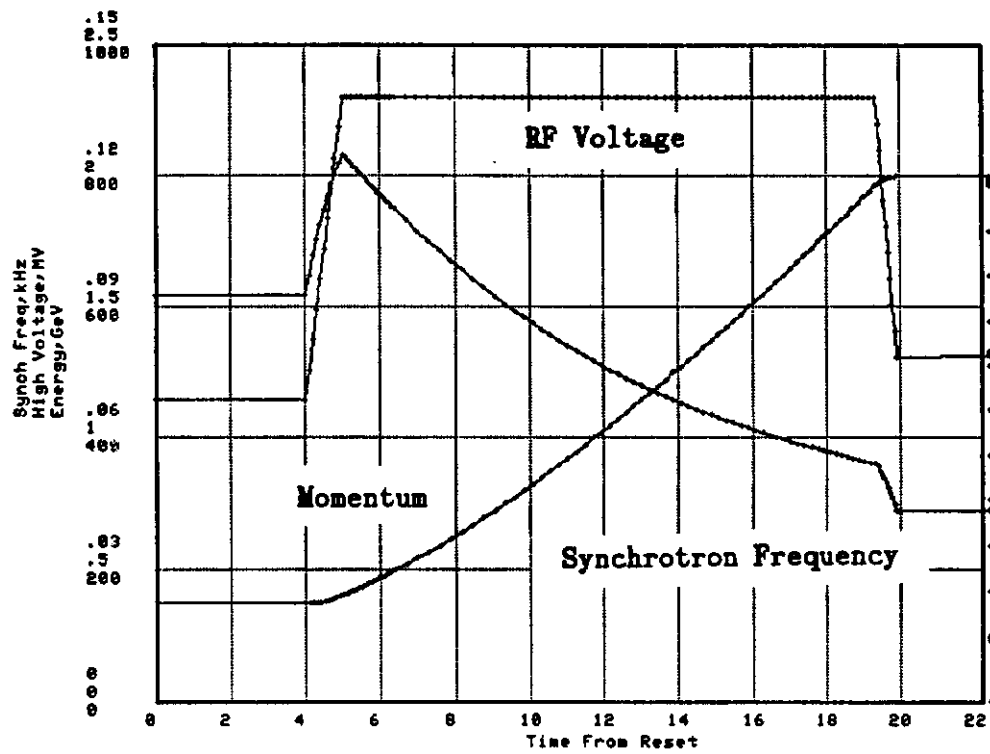


Figure 23: Plot of the Tevatron RF voltage, beam momentum, and small amplitude synchrotron amplitude during acceleration.